

Supporting information for:

Ultra-Low Percolation Threshold in Nano-Confined Domains

David R. Barbero* and Nicolas Boulanger

*Nano-Engineered Materials and Organic Electronics Laboratory,
Umeå Universitet, Umeå 90187, Sweden*

E-mail: david.barbero@umu.se

Mold Filling Mechanism

In order to better understand the reasons for vertical alignment of the nanotubes in the patterns, partial imprints were produced in order to visualize the nanoscale flow inside the mold cavities during imprinting. In this case, micro patterns were imprinted for only a few seconds in order to observe the filling mechanism of the partially filled cavity. The imprints were imaged using atomic force microscopy (AFM), as shown in Figure S1.

It can be seen that the polymer initially flows vertically along the mold cavities (Figure S1a-c), before filling the remainder of the mold, which is in agreement with previously published studies.^{S1,S2} During this process the nanotubes follow the flow of polymer, and therefore align vertically with the flow (Figure S1d), creating partially vertically aligned networks as confirmed by Raman spectroscopy (see Figure 3b,c). In the case of the 2D network however the nanotubes remain mostly in the plane of the film due to the spin coating process.

*To whom correspondence should be addressed

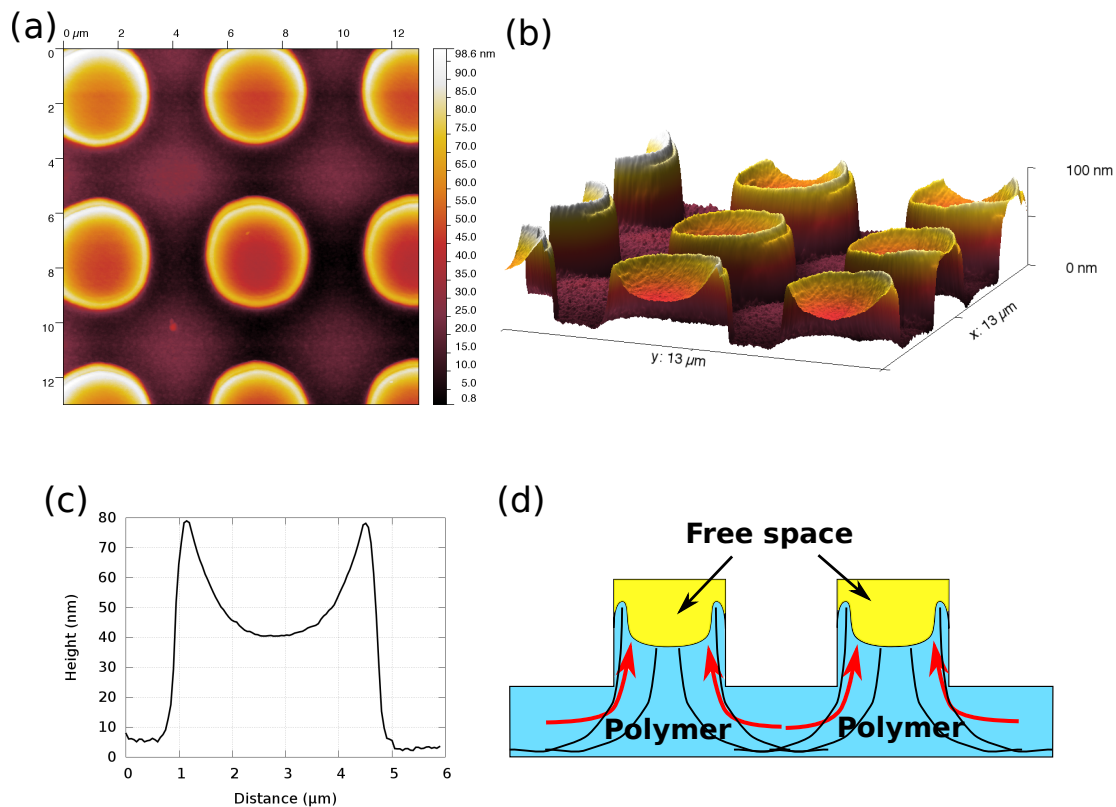


Figure S1: Partial micro imprint. Shown are (a) 2D and (b) 3D AFM pictures of a partially imprinted composite. (c) shows the profile of a partially imprinted pillar, while (d) shows the filling process during the imprinting. The patterns are filled progressively, starting from the edges of the mold, in the vertical direction.

The nanotubes follow the polymer flow during the imprinting process, and therefore align vertically within the patterns, creating vertical networks allowing for out of plane conductivity, while in the case of the random network, they remain mostly in the plane of the film due to the spin coating, and mostly favors in-plane electrical conductivity.

The mean shear rate of the polymer/SWNT viscous composite during mold filling was calculated using the following equation^{S3} :

$$\frac{d\gamma}{dt} = \frac{3 \cdot P \cdot h}{\eta \cdot s} \quad (1)$$

where P is the applied pressure, h is the initial film thickness, η is the composite viscosity, and s is the recessed pattern width of the mold. Here, the values of temperature (150°C) and pressure (15 bar) used were the same for the micro and the nano networks. The viscosity was also considered nearly identical because of the very low SWNT concentration used, and can be approximated to the viscosity of the polymer melt itself. Therefore any difference in shear rate must come from the values of h and s . A total thickness $h \approx 75$ nm and 390 nm, and values of $s \approx 430$ nm and 2000 nm were measured for the nano-patterns and for the micro-patterns respectively. Therefore the ratio (h/s) is ≈ 0.17 and 0.20 for nano and micro-patterns respectively, which represents $\approx 18\%$ increase in shear rate during formation of the micro confined patterns.

Effect of Confinement on ϕ_c

Figure S2 shows the effects of the confinement on the percolation threshold. The evolution of the percolation threshold is shown as a function of the volume of the composite (Figure S2a) over one unit area of period P . It can be seen that the percolation threshold decreases with a reduction in network size and volume. In Figure S2b and S2c for the same area (here a single period of the micro network) the volume occupied by the nano network (in yellow) is

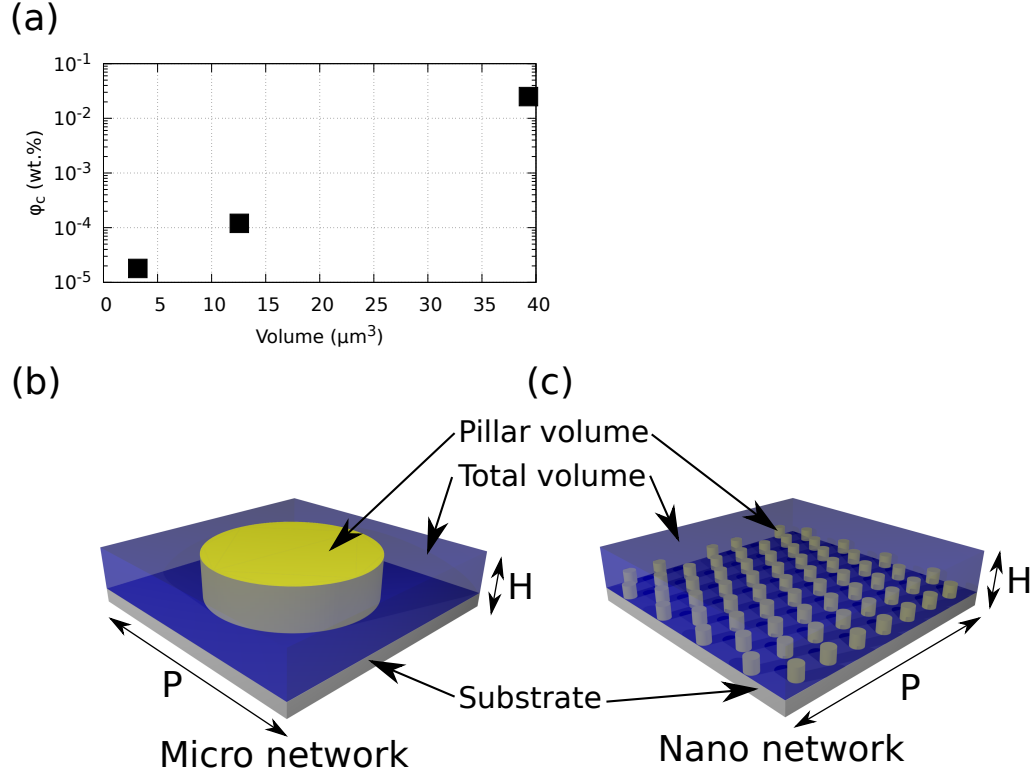


Figure S2: Influence of the confinement on the percolation threshold of the composites. (a) evolution of the percolation threshold as a function of the volume of material in each network; (b) volume occupied by the micro-network in one unit area of period P ; (c) shows the volume occupied by the nano pillars over the same area. In both (b) and (c), the actual volume of material (yellow) is defined as the volume occupied by the pillars contained in one unit area of period P .

smaller than the one occupied by the micro network, resulting in greater confinement of the nanotubes within the composite. The tube vertical alignment is almost identical (a little stronger in the micro-network) in both 3D networks (as determined by Raman measurements, Figure 3), however the volume occupied by the nano network is smaller than the one occupied by the micro network (in yellow in Figure S2b and S2c), resulting in greater confinement of the nanotubes within the composite. The smaller volume and increased confinement enable formation of conducting percolated pathways within the network at much lower loadings and with fewer contact resistances, thereby resulting in the reduction in ϕ_c observed.

Electrical Conductivity Measurement

Electrical conductivity was measured vertically, between the bottom of the sample to the top of the pillars as shown in Figure 2a. The bottom contact between the conducting, P-doped silicon and the brass plate is done using conducting silver paste. The top contact is achieved using a gold coated polydimethylsiloxane (PDMS) stamp. The flexibility of the PDMS allows for good contact with the top of the patterns, while avoiding contact with the residual layer in between them. A slight pressure (≈ 0.3 bar) was applied on the gold coated PDMS electrode to help produce good conformal contact, as previously demonstrated elsewhere.^{S4} A varying potential difference was then applied between the two contacts (top and bottom) and the resulting electrical current is measured.

Figure S3 shows the evolution of the measured current densities as a function of the applied voltage for a selection of samples for the different types of networks under study. Data is shown only for samples above the percolation threshold. It can generally be observed that the current follows a nearly ohmic behavior at low voltages (below 0.1 V) in all types of networks. At higher voltages the random network follows $J \propto V^\alpha$ where J is the current density, V the applied potential and α an exponent between ≈ 2.3 and 2.5. This change in behavior can be explained as follow: at low voltages, the electrical conduction is mainly due

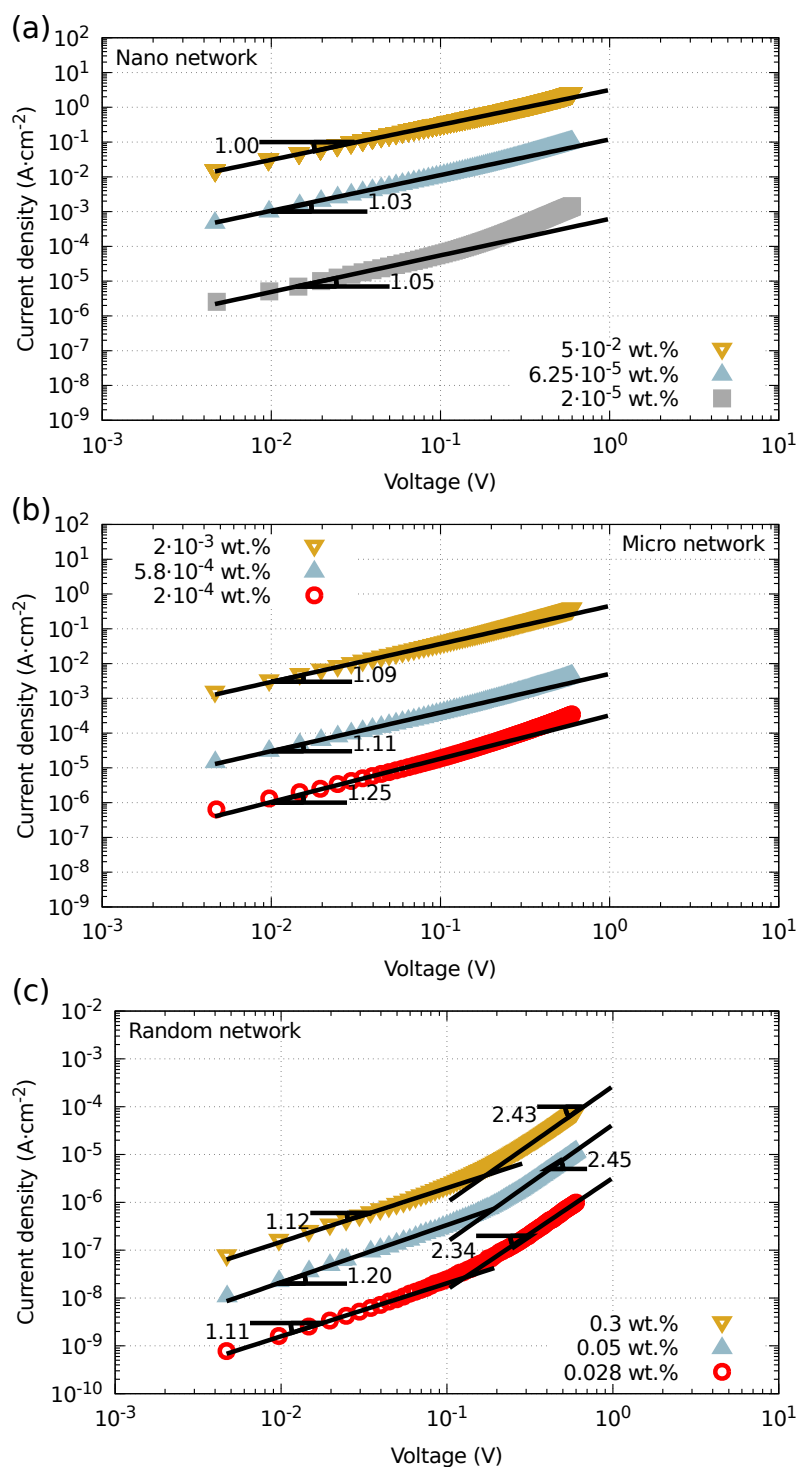


Figure S3: Current densities measured as a function of the applied potential for (a) nano networks, (b) micro networks and (c) random networks at different nanotube loadings. The slopes are fitted for both the low voltage and high voltage part of the plots, showing the change of behavior in the conductivity.

to tunneling effects, which leads to an almost linear variation of the current with the applied voltage (slope ≈ 1.0).^{S5,S6} At higher voltages, electron hopping effects appears, in addition to the tunneling current, resulting in higher slopes on the log-log J-V plots.^{S7} Interestingly, the current in the nano and micro networks still follows a quasi-ohmic behavior in the region where the random network deviates from this regime. The general increase in current density when the nanotube loading increases is explained by the increase in the number of pathways for the current to go through due to the increased network density within the composites.

References

- (S1) Jun, D.; Zhengying, W.; Huali, C.; Yubin, Z. Investigation of Resist Filling Profile Evolution in Microimprint Lithography. *J. Vac. Sci. Technol. B* **2015**, *33*, 011601.
- (S2) Wang, Q.; Hiroshima, H.; Suzuki, K.; Youn, S.-W. Real-Time Full-Area Monitoring of the Filling Process in Molds for UV Nanoimprint Lithography Using Dark Field Illumination. *J. Vac. Sci. Technol. B* **2012**, *30*, 06FB13.
- (S3) Schulz, H.; Wissen, M.; Bogdanski, N.; Scheer, H.-C.; Mattes, K.; Friedrich, C. Impact of Molecular Weight of Polymers and Shear Rate Effects for Nanoimprint Lithography. *Microelectron. Eng.* **2006**, *83*, 259–280.
- (S4) Skrypnichuk, V.; Wetzelaer, G.-J. A. H.; Gordiichuk, P. I.; Mannsfeld, S. C. B.; Herrmann, A.; Toney, M. F.; Barbero, D. R. Ultrahigh Mobility in an Organic Semiconductor by Vertical Chain Alignment. *Adv. Mater.* **2016**, *28*, 2359–2366.
- (S5) Biaye, M.; Zbydniewska, E.; Mélin, T.; Deresmes, D.; Copie, G.; Cleri, F.; Sangeetha, N.; Decorde, N.; Viallet, B.; Grisolia, J.; Ressier, L.; Diesinger, H. Tunneling Mechanism and Contact Mechanics of Colloidal Nanoparticle Assemblies. *Nanotechnology* **2016**, *27*, 475502.

- (S6) Simmons, J. G. Generalized Formula for the Electric Tunnel Effect Between Similar Electrodes Separated by a Thin Insulating Film. *J. Appl. Phys.* **1963**, *34*, 1793–1803.
- (S7) Feng, C.; Jiang, L. Y. Investigation of Uniaxial Stretching Effects on the Electrical Conductivity of CNT–Polymer Nanocomposites. *J. Phys. D: Appl. Phys.* **2014**, *47*, 405103.